

Controlled Dissolution of Crystals: Application to Berlinite (α AlPO₄), a Piezoelectric Material

O. CAMBON,¹ A. GOIFFON, A. IBANEZ, AND E. PHILIPPOT

Laboratoire de Physicochimie des Matériaux Solides, URA DO407 CNRS, Place E. Bataillon, UM II case 003, 34095 Montpellier Cedex 5, France

Received January 23, 1992; in revised form June 22, 1992; accepted October 6, 1992

This paper presents the controlled dissolution of berlinite, a new piezoelectric material. The first part of this work presents a short review of crystal growth and dissolution theory where only the major relations are taken into account and interpreted in view of their application in the controlled dissolution of berlinite crystals. The second part presents the results obtained for the chemical etching of berlinite in acid media. The composition of the etching bath was chosen to improve the surface state according to dissolution theory. © 1993 Academic Press, Inc.

Introduction

For the past several years industrial interest in piezoelectric materials has increased due to the development of telecommunication devices with filters made of piezoelectric resonators.

In the particular case of BAW (Bulk Acoustic Wave) devices, plate lapping is an important step in resonator manufacturing. This operation must produce a good surface state with a definite thickness that agrees with the required frequency. The minimum thickness attained by mechanical lapping is about 40 μm . To reach a thickness of about 15 μm it is necessary to use unconventional methods: ion beam etching (IBE) and chemical etching.

The IBE method is widely used in the quartz industry for high-frequency resonator

devices. Quartz is a well known and cheap material; however, the works devoted to devising an industrial method of quartz chemical etching using fluoride media have not been successful (1).

The aim of this work is to specify good chemical lapping conditions for a new piezoelectric material, berlinite (AlPO₄), in order to utilize it on an industrial scale. Previous studies (2, 3) have shown that acids used as crystal growth media, i.e., phosphoric, sulfuric, and hydrochloric acids, can be utilized as etching solvents. Nevertheless, these acids do not produce a good surface state.

Therefore, in order to verify and to better understand the dissolution process, it is necessary to go back to the basic theory of crystal growth and dissolution. After taking these theories into account, some chemical etching methods have been proposed which give accurate thickness with very smooth surface state.

¹ Present address: C.E.P.E./Thomson, 44 avenue de la Glacière, B.P. 165, 95100 Argenteuil Cedex, France.

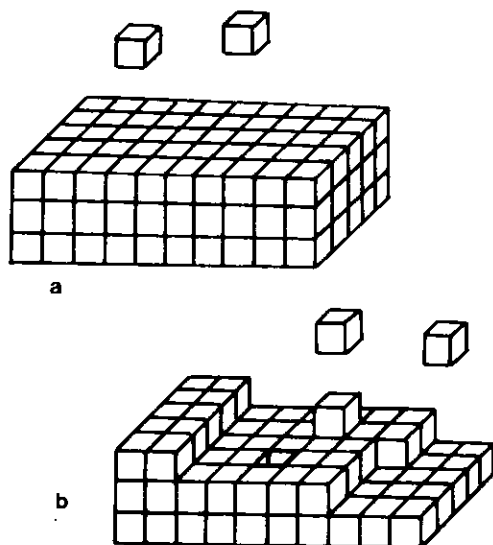


FIG. 1. (a) Perfect crystal. (b) Real crystal.

Crystal Growth and Dissolution Phenomenon Theory

Before undertaking a controlled dissolution process for berlinite, we perfected the crystal growth of this material (4). After this we were interested in the reciprocal characteristic of the crystal growth theory inasmuch as both crystal growth and crystal dissolution follow the same thermodynamic relation.

Since Gibbs (5), most work has been applied first to the growth of perfect crystals (6–8), and subsequently to the growth of real crystals from vapor phases (9, 10) or in solutions (11, 12). Recently, this theory has been extended to the reverse process for perfect and real crystals; i.e., the dissolution mechanism (13–15).

Growth kinetics depend mostly on the solute entity probability of reaching the crystal surface. This probability of absorption is increased by the existence of propitious sites creating bonds with the solute particles. Therefore, the crystal–solution interface structure becomes important in the crystal growth process. Figure 1 schematizes

smooth and rough faces of ideal and real crystals; the bonding probability is higher in the second case. This difference explains why strong (13) and weak (10) supersaturations are needed for perfect and real crystal growth, respectively. Therefore, perfect crystals need 50% supersaturation for ideal crystal growth (13).

The free energy change needed for the formation of a nucleus on a perfect surface can be expressed through the relation (10)

$$\Delta G_p = \frac{\pi r a^2}{\Omega} kT \ln \frac{C}{C_0} + 2\pi r a \gamma, \quad (1)$$

where r and a are the radius and nucleus height, respectively, Ω is the solute molar volume, γ the crystal–solution surface energy, C the material concentration in the solution, and C_0 its solubility at temperature T (°C). Then, the critical size of the nucleus, r^* , is derived by $d(\Delta G_p)/dr = 0$, and the final equation is:

$$r^* = \frac{\Omega \gamma}{kT \ln C/C_0} \quad (2)$$

The corresponding activation energy (ΔG_p^* when $r = r^*$) for nucleation on a perfect surface is written as

$$\Delta G_p^* = \frac{\pi \gamma^2 \Omega a}{kT \ln C/C_0}. \quad (3)$$

For real crystals (9, 10), the free energy change for nucleus formation at a dislocation requires an additional term of “strain energy,” $E(r)$, and is written as

$$\Delta G_d = \frac{\pi r^2 a}{\Omega} kT \ln \frac{C}{C_0} + 2\pi r a \gamma - a E(r). \quad (4)$$

If $E(r)$ has a positive value, the free energy change for nucleus formation for a real crystal at a dislocation is less than that for a perfect crystal. ΔG_p and ΔG_d free energy variations have been compared (15) and it has been confirmed that nucleation activa-

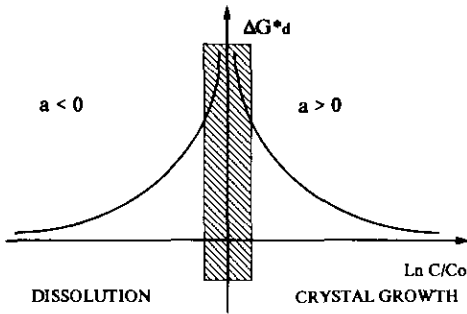


FIG. 2. ΔG_d^* energy barrier variation for growth and dissolution of a real crystal in terms of solute concentration, C (C_0 = solubility).

tion energy at critical radius ΔG_d^* is lower than that of ΔG_p^* .

For the reverse process, i.e., the dissolution process, the same relationship is used to describe perfect crystal dissolution, as well as real crystal dissolution. The only difference is the assignment of a positive or negative value of the "a" parameter based on the height of the nucleus or the depth of the pit.

For a real crystal, surface defects favor preferential dissolution. If the undersaturation is too great (low C/C_0 and $\Delta G_d^* \cong 0$; i.e., no energy barrier), dislocation cores "open up" spontaneously and lead to etch pit and etch channel formation. Hence, to avoid this formation, the solutions must be only slightly undersaturated (15).

Material dissolution in the solutions increases the energy barrier, thus preventing etch pit formation. Unfortunately, if the energy barrier is too high, the etching rate will be drastically slowed, and hence a middle course must be found. Figure 2 schematizes the ΔG_d^* energy barrier variation for growth and dissolution for a real crystal. The hatched part idealizes the high ΔG_d^* zone and this condition is used to produce a very good crystalline quality in the growth process or a controlled dissolution process without etch pit formation. Nevertheless,

crystal growth and etching rates decrease when $C \rightarrow C_0$; i.e., the system is in equilibrium.

Another simplification of the behavior of a real crystal from a structural defect is shown in Fig. 3. The etching rate can be expressed in terms of two components (14) giving the pit profile evolution, with V_N , the normal rate to the surface, and V_S , the parallel rate to the surface.

If $V_N > V_S$, deep pits (etch pits and etch channels) will form, whereas if $V_S > V_N$, shallow ones will prevail. The V_S rate, and consequently the etch pit profile, is influenced by the solute concentration of the etching baths (15).

All these considerations confirm the cardinal importance of the degree of solution saturation, both for crystal growth and for the dissolution process. In the next sec-

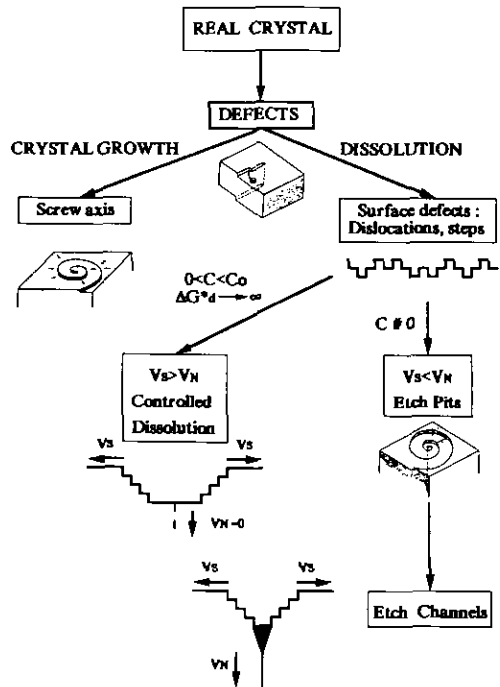


FIG. 3. Simplification of the behavior of a real crystal from a structural defect.

tion, these results will be discussed for dissolution of berlinite, AlPO_4 .

Application to the Dissolution of a Piezoelectric Material: Berlinite (AlPO_4)

Berlinite is a new piezoelectric material with a quartz structure. The new generation of telecommunication devices needs piezoelectric compounds like berlinite which present thermally compensated orientations and a piezoelectric coupling coefficient better than those of quartz ($k \approx 11\%$ for AT, a temperature compensated cut near $Y-33^\circ$). Berlinite is a compound adapted for BAW devices.

This work is devoted to AT-cut berlinite plates and is an extension of our previous papers dealing with chemical etching in pure H_2SO_4 (2) and with mechanism's dissolution in acid media (16).

After a short review of berlinite dissolution in acid media ($C = 0$), the results of dissolution in ($\text{AlPO}_4 + \text{acid}$) media are determined and compared to conclusions deduced from the theory presented above.

Last, some berlinite chemical lapping resonators have been made and piezoelectrically characterized.

Samples, Experimental Procedure, and Characterization Methods

Berlinite crystals were synthesized under experimental crystal growth conditions perfected in our department (4). Ground and polished AT-cut disks were 5 mm in diameter. Two sizes of final abrasive were used, 3 μm for ground wafers and 0.3 μm for polished wafers.

The used plates were 150 or 70 μm thick before chemical etching. These thicknesses correspond to resonance frequencies of about 10 and 21 MHz, respectively.

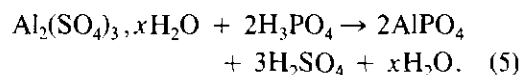
Etching Procedure

The experimental procedure has been described elsewhere (3). Etching solutions

were prepared by diluting commercial acids. Concentrations were checked by densimetry and typical acid-base analysis. When the solute concentration was not zero, different preparation methods were used which are summarized below:

—Phosphoric acid medium: solutions of $\text{H}_3\text{PO}_4 + \text{AlPO}_4$ were prepared from berlinite, aluminum hydroxide, or commercial aluminum phosphate.

—Sulfuric acid medium: two methods were used to prepare the ($\text{H}_2\text{SO}_4 + \text{AlPO}_4$) solutions; dissolution of berlinite crystals in sulfuric acid and dissolution of hydrated aluminum sulfate in phosphoric acid, according to the reaction



Control Methods

Chemical etching has been controlled by:

—thickness measurements of plates by frequency measurements

$$F(\text{MHz}) = K/e \quad (6)$$

where e is the plate thickness given in micrometers and K a constant relating to the material and orientation studied ($K = 1480 \text{ MHz } \mu\text{m}$ for the berlinite AT cut).

—Surface texture characterization has been made by defining the R_a parameter derived from roughness measurements and microscopy observations.

Experimental Results and Discussion

Two different kinds of results have been obtained and depend on the berlinite concentration in the etching solutions; $C = 0$ and $C \neq 0$.

Chemical Etching in Pure Acidic Media (H_2SO_4 , HCl , H_3PO_4) ($C = 0$)

Etching rates have been measured in these acid solutions and we have determined

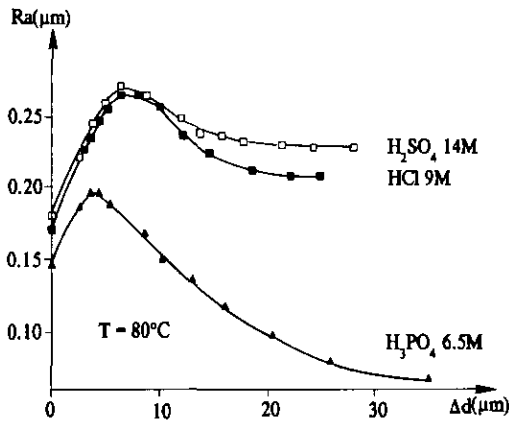


FIG. 4. Ra parameter variation of berlinite AT plates versus plate thickness decrease: (a) H_2SO_4 14 M and $T = 80^\circ C$. (b) HCl 9 M and $T = 80^\circ C$. (c) H_3PO_4 6.5 M and $T = 80^\circ C$.

only one kinetic equation and one dissolution mechanism for all these acid media (16):

$$V = A \exp(-Ea/RT)[H^+]^{1/2}. \quad (7)$$

In Fig. 4, the Ra parameter variation is reported versus plate thickness decrease for the three acids studied. All ground samples used had an initial average roughness value of $Ra \approx 0.15 \mu m$, presenting the same maximum roughness behavior with a decrease in the thickness value of about $6 \mu m$. After that, the average roughness gradually decreased.

The first part of the curves (when the roughness increases) corresponds to the chemical etching of the superficial layer disturbed by the cutting and initial grinding. Then, the roughness decrease is the intrinsic phenomenon of chemical lapping. It can be observed that the surface state obtained in phosphoric acid is better ($Ra \approx 0.05 \mu m$) than that obtained with sulfuric or hydrochloric acid ($Ra \approx 0.2 \mu m$).

These measurements were confirmed by microscopy observations (3). It was observed that the phosphoric acid leads to better surface texture and less etch pit forma-

tion than the sulfuric one. Even if the solute concentration is zero, we can assume that this improvement is due to the presence of the PO_4^{3-} anion.

Chemical Etching in Acid Media (H_2SO_4 , H_3PO_4) with Dissolved $AlPO_4$ ($0 < C < C_0$)

Sulfuric acid medium. Some experimental etching rates in ($H_2SO_4 + AlPO_4$) media have been shown in Table I and compared to those calculated in pure sulfuric acid solutions. We can observe that the increase of berlinite concentration induces a significant etching rate decrease.

In this case, the etching rate cannot be expressed only in terms of $[H^+]$ concentration alone, as for pure acid solutions, but must take aluminum phosphate concentration into consideration. This term decreases the dissolution kinetics to zero when $C = C_0$.

The surface texture has been checked by roughness measurements and microscopy observations. Ra parameter variation is given in Fig. 5 and it can be observed that an increasing value of the $AlPO_4/H_2SO_4$ ratio strongly improves the final surface state. Nevertheless, even if the final Ra value of $0.05 \mu m$ is estimated as good lapping, the presence of some etch pits, even in the best cases, can be observed.

TABLE I

CALCULATED ETCHING RATES IN PURE SULFURIC ACID MEDIUM COMPARED TO EXPERIMENTAL ONES IN SULFURIC ACID + ALUMINUM PHOSPHATE MEDIUM

T ($^\circ C$)	H_2SO_4		$H_2SO_4 + AlPO_4$	
	(M)	V_{cal} ($\mu m/h$)	(M)/(M)	V_{obs} ($\mu m/h$)
90	8	15.7	8/3.6	3.4
80	5.25	6.1	5.25/3.5	2.3
90	5.25	11.0	5.25/3.5	4.4

Note. Computed values are determined from kinetics equation previously indicated.

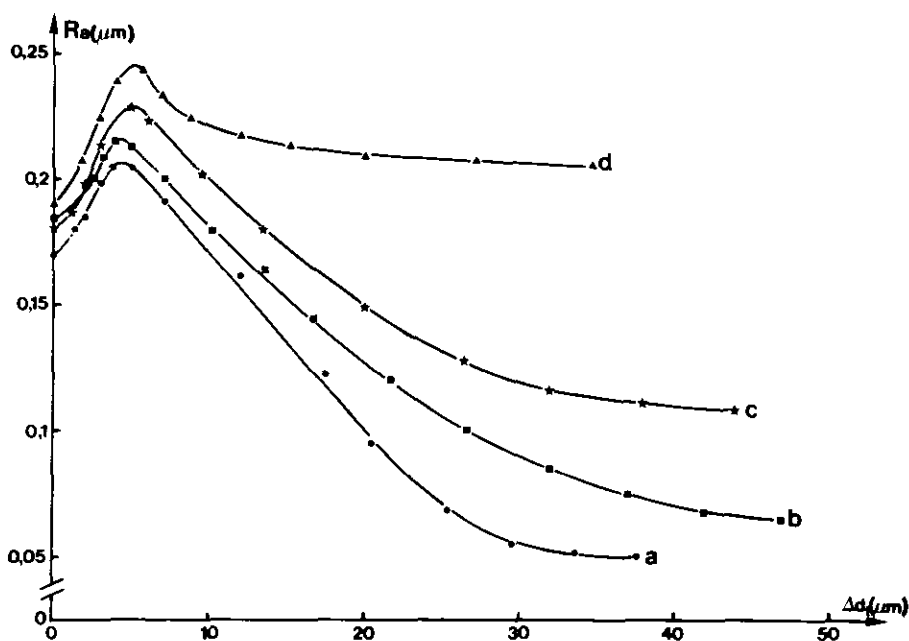


FIG. 5. Berlinite concentration influence on Ra parameter evolution in sulfuric acid medium at 90°C . a, $(\text{AlPO}_4)/(\text{H}_2\text{SO}_4) = 0.66$; b, $(\text{AlPO}_4)/(\text{H}_2\text{SO}_4) = 0.45$; c, $(\text{AlPO}_4)/(\text{H}_2\text{SO}_4) = 0.25$; d, $(\text{AlPO}_4)/(\text{H}_2\text{SO}_4) = 0.04$.

Improvement of surface texture for high C/C_0 ratio, outside etch pit zones, can be followed by light microscopy as is shown in Photo 1. Photo 2 gives an idea of the etch pit presence concentration.

In brief, for $(\text{H}_2\text{SO}_4 + \text{AlPO}_4)$ solutions, polishing effects are significantly improved when the AlPO_4 concentration increases. This observation can be explained in the light of crystal growth and dissolution theory: the C/C_0 ratio is still far from 1 and thus the energy barrier ΔG_a^* is not high enough to avoid etch pit formation (at least for the crystalline quality of the samples used in this study).

In view of the very different results obtained in pure sulfuric and phosphoric acid solutions, we have undertaken to check the behavior of berlinite dissolution in $\text{H}_3\text{PO}_4/\text{AlPO}_4$ acid media.

Phosphoric acid medium. Some typical results relating to dissolution kinetics in

$(\text{H}_3\text{PO}_4 + \text{AlPO}_4)$ solutions are reported in Table II. As observed in sulfuric acid media, etching rates of berlinite decreased when aluminum phosphate was added.

For surface texture, some characteristic roughness measurements have been shown in Fig. 6. Aluminum phosphate dissolved in phosphoric acid improves the final surface state significantly to a value of $Ra \cong 0.05 \mu\text{m}$, with (in contrast to sulfuric acid medium) etch pit vanishing, as in Photo 3. Furthermore, the Ra decrease can be observed even during the disturbed superficial layer etching and confirms the very good polishing effect from the phosphoric acid medium. Finally, if polished samples are used, Fig. 6c, with a starting value of $Ra \cong 0.01 \mu\text{m}$, this roughness is maintained along all the lapping. Taking all this into consideration, these $(\text{H}_3\text{PO}_4 + \text{AlPO}_4)$ solutions are the best ones for industrial device purposes.

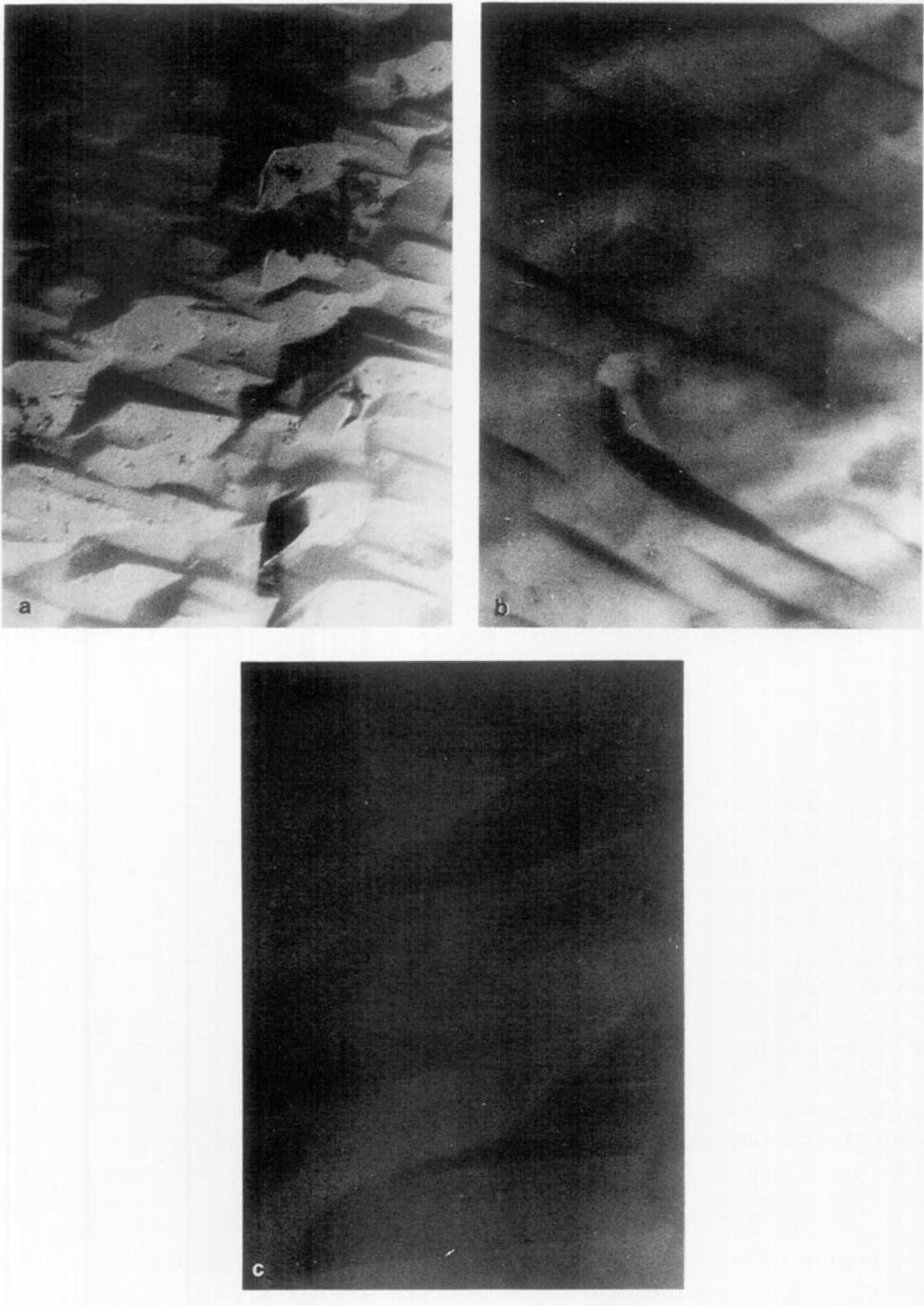


PHOTO 1. Surface texture evolution of AT cut during its chemical etching in a H_2SO_4 (8M) + AlPO_4 (3.6 M) solution at $T = 90^\circ\text{C}$ ($\times 330$). (a) $\Delta d = 13.5 \mu\text{m}$, $Ra = 0.165 \mu\text{m}$; (b) $\Delta d = 38 \mu\text{m}$, $Ra = 0.08 \mu\text{m}$; (c) $\Delta d = 47 \mu\text{m}$, $Ra = 0.06 \mu\text{m}$.

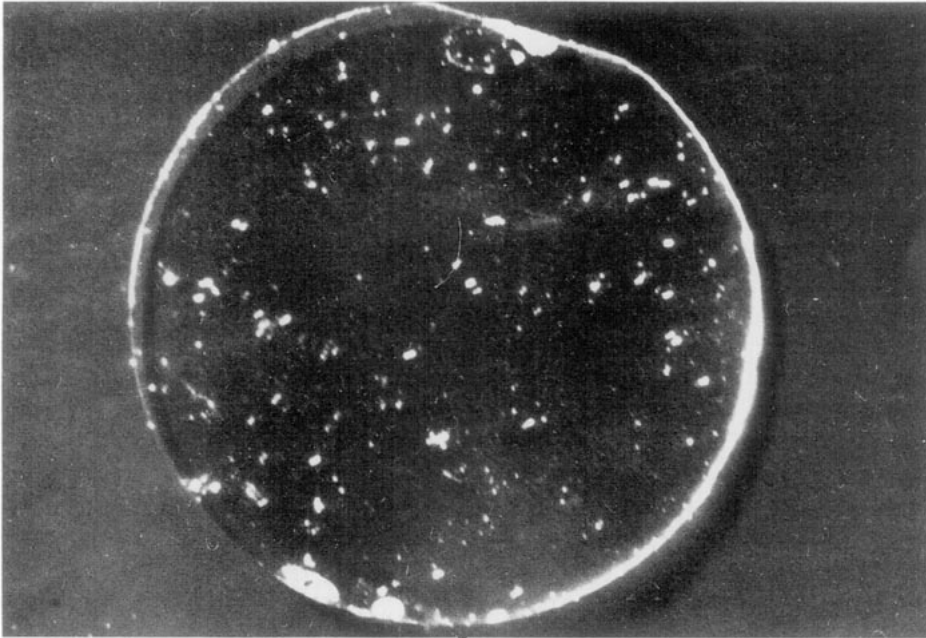


PHOTO 2. Surface texture of an AT cut showing some etch pits after 25 μm removal in a H_2SO_4 (5 M) + AlPO_4 (3.5 M) solution at $T = 80^\circ\text{C}$ ($Ra = 0.07 \mu\text{m}$).

For high-frequency resonator devices, surface state quality as well as thickness accuracy, which determines the resonance frequency, are of utmost importance. Thus, it is necessary to know accurately the etching rate equation in terms of different parameters. For aluminum phosphate acid solu-

tions, the etching rate equation must be expressed in terms of the concentration of all chemical entities in the solutions. This problem is very complicated. Nevertheless, new measurements are in progress for other acid and phosphate concentrations in order to determine a corresponding kinetics equation.

TABLE II

CALCULATED ETCHING RATES IN PURE PHOSPHORIC ACID MEDIUM COMPARED TO EXPERIMENTAL ONES IN PHOSPHORIC ACID + ALUMINUM PHOSPHATE SOLUTIONS

T ($^\circ\text{C}$)	H_3PO_4		$\text{H}_3\text{PO}_4 + \text{AlPO}_4$	
	(M)	$V_{\text{cal.}}$ ($\mu\text{m}/\text{h}$)	(M)/(M)	V_{obs} ($\mu\text{m}/\text{h}$)
90	9	83.7	9/2.7	36.3
70	9	44.6	9/2.7	22.5
70	10.4	51.0	10.4/3.5	11.2

Piezoelectric Characterization of Resonators Made from Chemical Lapping

Some samples, initially polished, have been chemically etched to increase the resonance frequency. Piezoelectric results are presented here (Tables III and IV). Two kinds of measurements have been undertaken:

(1) *Air-gap method.* The air-gap method is a technique well adapted to the chemical etching process because sample measurements can be taken without adhesive metal-

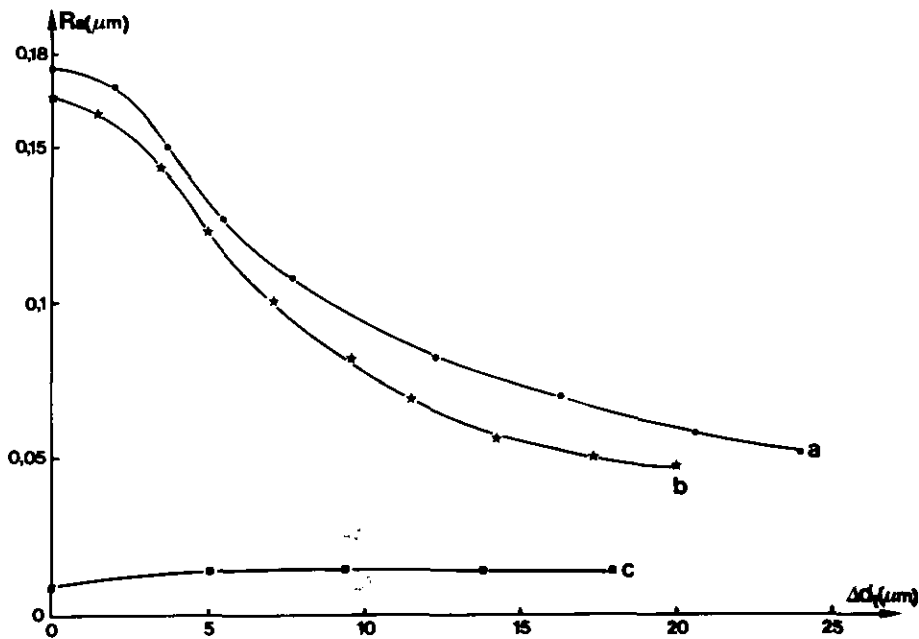


FIG. 6. Berlinite concentration influence on R_a parameter evolution in phosphoric acid medium at 80°C . (a) H_3PO_4 9 M/ AlPO_4 2.7 M; (b) H_3PO_4 6.5 M/ AlPO_4 3.2 M; (c) H_3PO_4 9 M/ AlPO_4 2.7 M.

lic electrodes throughout the etching process. The samples are put on an electrode with a diameter lower than the sample one and a small electrode is placed near the plate surface with an air gap. Some results from this method are given in Table III. Though they are not representative of the real quality of the plates, they allow an evaluation of the surface texture evolution during chemical etching, Fig. 7. In this example, after removal of $36 \mu\text{m}$, a Q factor value of 40,000 at 29 MHz ($QF = 1.17 \times 10^{12}$) confirms good etching conditions. Nevertheless, to have an accurate idea of the etching result, it is necessary to make resonators with adhesive electrodes.

(2) *Resonator measurements.* Square metallic electrodes are deposited on the two faces of the plates by evaporating techniques. Electrode dimensions must be adapted to the sample frequency measured, e.g., $\approx 0.4 \times 0.4 \text{ mm}^2$ for a 5-mm diameter

resonator at $\approx 75 \text{ MHz}$. These electrodes are connected to a network analyzer. By this method the real quality of the sample is evaluated. Different parameters of the resonator can be reached: the resonance frequency F_r , the resistance R , the self-inductance L , and the surtension factor Q (or the factor $Q \cdot F_r$), Table IV.

Before etching, the plate frequencies are measured by the air-gap method. After chemical etching, the samples are metallized to measure the different resonator parameters. Figure 8 gives an example of a 75-MHz-resonator result, after more than $50 \mu\text{m}$ has been removed. The Q factor value of 18,000 ($QF = 1.0 \times 10^{12}$) is close to that of an ion-beam etching.

These piezoelectric results show that the surface state reached by chemical etching is sufficient to make BAW devices. Nevertheless, the results, still not sufficiently reproducible, show that the crystalline quality

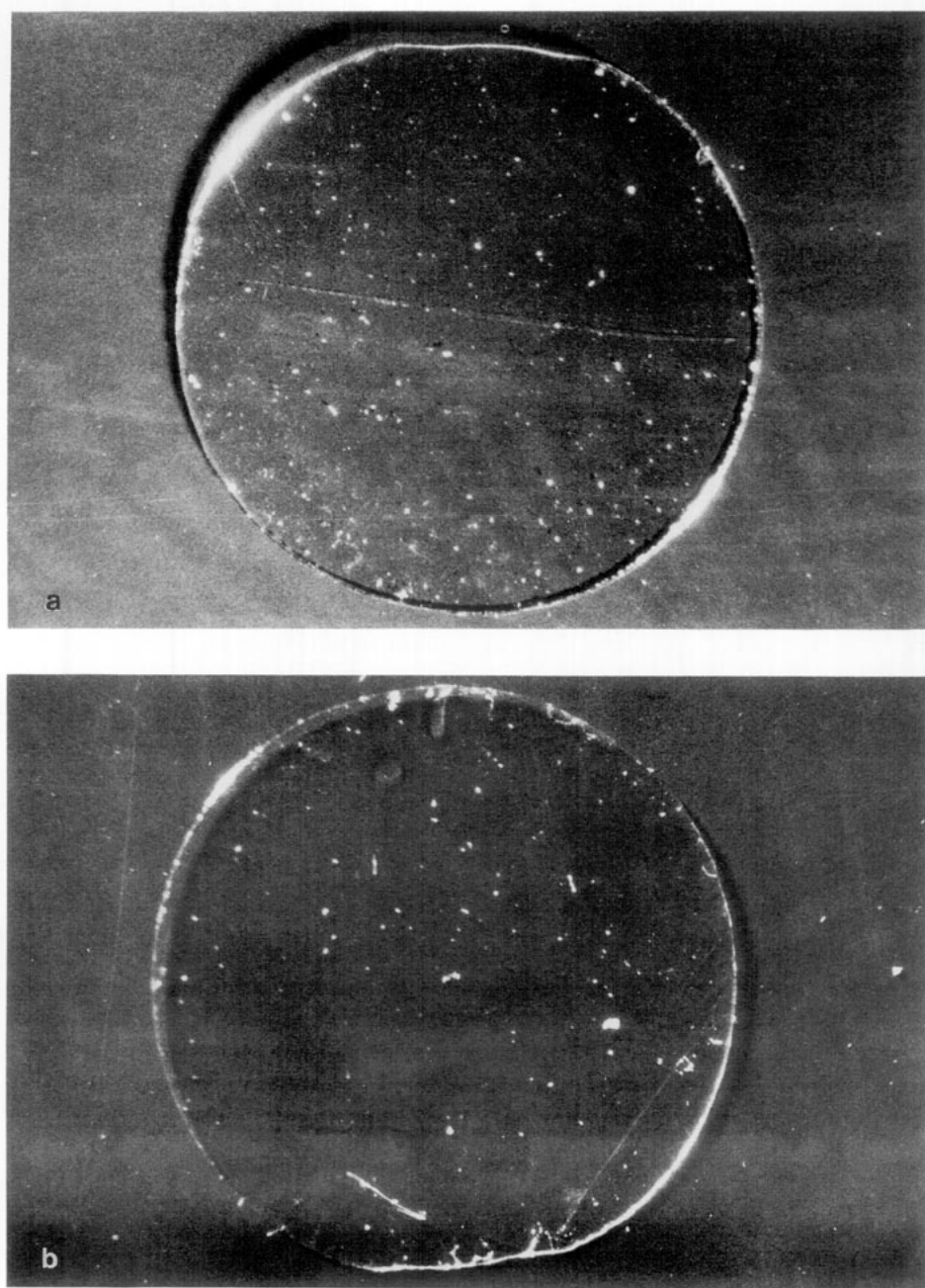


PHOTO 3. Chemical etching of polished sample in a H_3PO_4 (9 M) + AlPO_4 (2.7 M) solution at $T = 80^\circ\text{C}$: (a) before etching, $F = 20.9$ MHz ($e = 70.5$ μm), $Ra = 0.01$ μm ; (b) after etching, $F = 44.8$ MHz ($e = 33$ μm), $Ra = 0.015$ μm . White points are due to incomplete cleaning and not to etch pit formation.

TABLE III
F_r MEASUREMENT BY AIR-GAP METHOD

Before etching			Etching conditions			After etching		
<i>F_r</i> (MHz)	<i>e</i> (μm)	FIG.	[H ₃ PO ₄] (M)	[AlPO ₄] (M)	<i>T</i> (°C)	<i>F_r</i> (MHz)	<i>e</i> (μm)	Fig.
17.3	85.6		7.5	2.5	60	40.35	36.7	
19.5	76		7.5	2.5	60	39.2	37.7	
17.24	85.8		9	2.3	55	29.9	49.45	
16.9	87.5		9	2.3	55	27.8	53.2	
16.95	87.3	7a	9	2.3	65	29.1	50.8	7b

is not homogeneous enough in terms of different groups of crystal.

In conclusion, this etching process cannot succeed if plates present too many defects and, therefore, the major problem is improving the reliability of berlinite crystalline quality.

Conclusion

Before undertaking experimental aspects of berlinite lapping, and after seeing numerous failures encountered in quartz etching, we first considered using the etching method to obtain a good surface texture without etch pit formation and with accurate thickness.

From previous work, it appears that crystal growth and crystal dissolution are controlled by the same law. In both cases, to avoid all defects, it is necessary to create a

high energy barrier. This energy barrier is increased when solute concentration, *C*, draws nearer to material solubility, *C*₀, in the solvent studied.

In the case of a berlinite AT cut, Fig. 9 summarizes the most characteristic results of surface texture roughness in all studied media and confirms the very important role of solute concentration. Four different cases can be considered:

(1) Pure acid solutions (H₂SO₄, HCl), *C* = 0: the energy barrier is too weak to avoid high density of etch pits and etch channel formation. The final texture is worse than the starting texture.

(2) Pure phosphoric acid solutions, where *C* is still equal to zero: a strong improvement of the surface texture, but etch pit formation can be observed. This polishing effect of phosphoric acid has been assigned to the high concentration in these solutions of one

TABLE IV
SOME EXAMPLES OF RESONATOR MEASUREMENT AFTER CHEMICAL ETCHING

Before etching		Etching conditions			After etching					Fig.
<i>F_r</i> (MHz)	<i>e</i> (μm)	[H ₃ PO ₄] (M)	[AlPO ₄] (M)	<i>T</i> (°C)	<i>F_r</i> (MHz)	<i>e</i> (μm)	<i>R</i> (Ω)	<i>L</i> (μH)	<i>Q</i> · <i>F_r</i> (× 10 ¹²)	
20.9	70.6	10.4	2.7	70	44.2	33.5			0.2	
20.5	72.2	6	2.5	80	75	19.7	73.4	2015	1	8
20.2	73.3	6	2.5	80	77.1	19.2	55.3	1894	1.3	

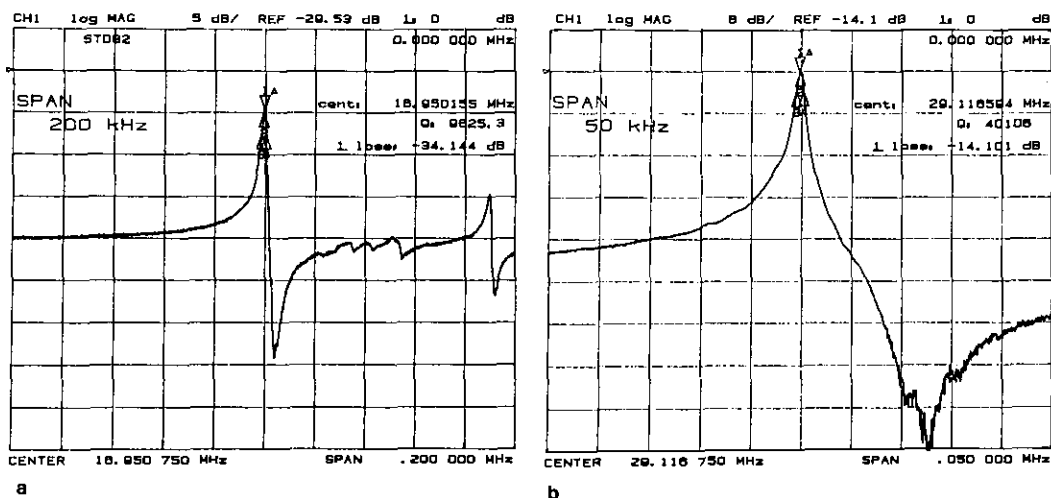


FIG. 7. Air-gap measurement of an AT berlinite plate before (a) and after (b) chemical etching.

of the component groups of the material: PO_4^{3-} anions.

(3) Acid solutions (H_2SO_4 , HCl , . . .) containing dissolved AlPO_4 : the energy barrier, due to the solute concentration, increases but is not sufficient to completely

avoid etch pit formation for crystalline quality of samples used. Nevertheless, it is possible to use this media for good crystalline quality cases.

(4) Phosphoric acid solutions containing AlPO_4 combine the advantages of both the previous cases to give the best lapping conditions for berlinite; i.e., a very smooth surface texture without etch pit formation.

Under these conditions, the last case is, by far, the best to use on an industrial scale and confirms the important role of solute concentration. As it is necessary to have a very slight supersaturation to have good crystal growth, the controlled dissolution of a material without defects requires light undersaturation of this material in its solvent.

To expand this investigation a systematic study has been undertaken to determine an accurate equation for the etching rate in terms of H_3PO_4 and AlPO_4 concentrations. On the other hand, it also should be possible to extend this to the controlled dissolution process for many other kinds of materials.

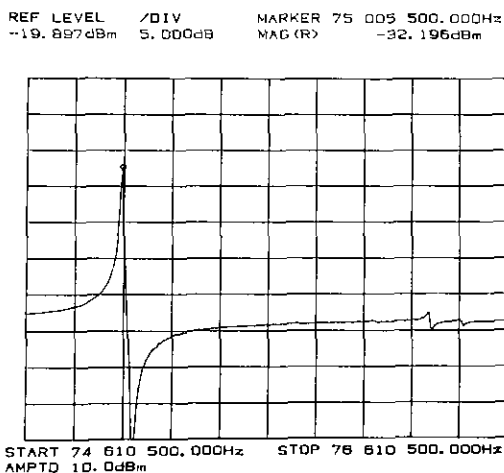


FIG. 8. Resonator measurement of a sample after chemical etching.

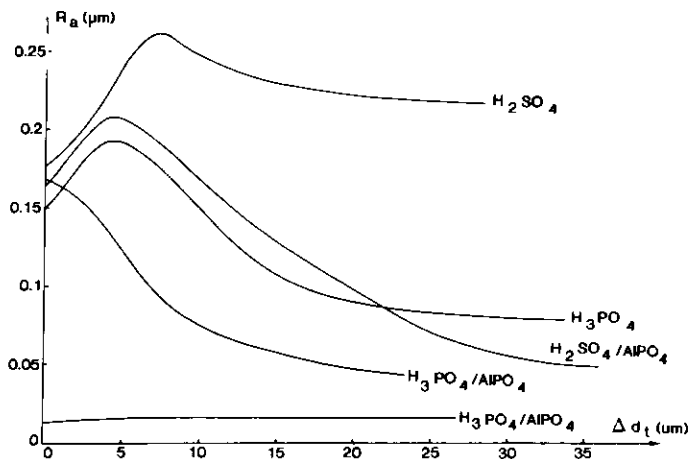


FIG. 9. Summary of the most characteristic results of surface texture roughness in all studied media.

Acknowledgments

The authors acknowledge the C. N. R. S. and the C.E.P.E./Thomson Company, Argenteuil, France, for their financial support.

References

1. C. R. TELLIER, *J. Mater. Sci.* **17**, 1348 (1982); C. R. TELLIER, *Surf. Technol.* **21**, 83 (1984); C. R. TELLIER, N. VIALLE, AND J. L. VATERKOWSKI, "1st Europ. Freq. and Time Forum, Besançon," (1987); J. R. BRANDMAYR AND J. R. VIG, "40th Annual Freq. Control. Symp.," (1986).
2. O. CAMBON, A. GOIFFON, E. PHILIPPOT, J. P. AUBRY, AND J. DETAINT, "4th Eur. Freq. Time Forum," pp. 601 (1990).
3. O. CAMBON, A. GOIFFON, AND E. PHILIPPOT, *J. Mater. Sci.* **26**, 846 (1991).
4. E. PHILIPPOT, A. GOIFFON, M. MAURIN, J. DETAINT, J. SCHWARTZEL, Y. TOUDIC, B. CAPELLE, AND A. ZARKA, *J. Cryst. Growth* **104**, 713 (1990).
5. J. W. GIBBS, "Collected Works, 1928," Vol. 1, p. 325, Longmans, Green, and Co., New York.
6. W. KOSSEL, *Nachr. Ges. Wiss. Göttingen*, 135 (1927).
7. I. N. STRANSKI, *Z. Phys. Chem.* **136**, 259 (1928).
8. J. FRENKEL, *J. Phys. USSR* **9**, 392 (1945).
9. W. K. BURTON, N. CABRERA, AND F. C. FRANK, *Nature* **163**, 398 (1949).
10. W. K. BURTON, N. CABRERA, AND F. C. FRANK, *Philos. Trans. R. Soc. London* **243**, 299 (1951).
11. P. BENNEMA, *J. Cryst. Growth* **1**, 278 (1967).
12. P. BENNEMA AND G. H. GILMER, *J. Cryst. Growth* **13**, 148 (1972).
13. W. K. BURTON AND N. CABRERA, *Disc. Faraday Soc.* **5** (1949).
14. W. G. JOHNSTON, *Prog. Ceram. Sci.* **2**, 1 (1962).
15. (a) N. CABRERA AND M. M. LEVINE, *Philos. Mag.* **1**, 450 (1955); and (b) N. CABRERA, M. M. LEVINE, AND J. S. PLASKETT, *Phys. Rev.* **96**, 1153 (1954).
16. O. CAMBON, A. GOIFFON, A. IBANEZ, AND E. PHILIPPOT, *Eur. J. Solid State Inorg. Chem.* **29**, 547 (1992).